# Adaptive feedback control of ultrafast semiconductor nonlinearities

J. Kunde,[a] B. Baumann, S. Arlt, and F. Morier-Genoud
*Ultrafast Laser Physics, Institute of Quantum Electronics, Swiss Federal Institute of Technology,*
*ETH Hoenggerberg HPT, CH-8093 Zurich, Switzerland*

U. Siegner
*Physikalisch–Technische Bundesanstalt, Bundesallee 100, D-38116 Braunschweig, Germany*

U. Keller
*Ultrafast Laser Physics, Institute of Quantum Electronics, Swiss Federal Institute of Technology,*
*ETH Hoenggerberg HPT, CH-8093 Zurich, Switzerland*

We experimentally demonstrate that adaptive feedback optical pulse shaping can be used to control ultrafast semiconductor nonlinearities. The control scheme is based on an evolutionary algorithm, which directs the modulation of the spectral phase of 20 fs laser pulses. The algorithm has optimized the broadband semiconductor continuum nonlinearity measured in differential transmission experiments. Our results show that insight into light–semiconductor interaction is obtained from the optimum laser pulse shape even if the interaction is too complex to predict this shape *a priori*. Moreover, we demonstrate that adaptive feedback control can substantially enhance ultrafast semiconductor nonlinearities by almost a factor 4. © *2000 American Institute of Physics.*
[S0003-6951(00)00733-6]

In recent years, ultrafast semiconductor optical nonlinearities have been the subject of extensive research.[1] The complexity of the physics involved[1,2] makes it still very difficult to reliably predict *a priori* the exact optical pulse shape that produces a desired nonlinear response. Therefore, ultrafast semiconductor nonlinearities are an ideal arena for adaptive feedback optical pulse shaping. The usefulness of feedback schemes has been demonstrated for optical pulse compression,[3,4] for the synthesis of predefined pulses shapes,[5] and for the control of molecules,[6–8] and of the quantum wave function of atoms.[9]

In this letter, we experimentally demonstrate that adaptive feedback optical pulse shaping can be used to control ultrafast semiconductor nonlinearities. Our work focuses on the broadband semiconductor continuum nonlinearity, which will play a key role in future ultrafast semiconductor devices, rather than the narrowband excitonic nonlinearity. Our data demonstrate that knowledge of the optimum pulse shape gives *a posteriori* insight into the interaction of semiconductors and ultrafast optical pulses. Specifically, we develop an intuitive picture of the complex photon-energy dependence of carrier relaxation in the thermalization regime. These results show the potential of adaptive feedback control as a technique in ultrafast semiconductor spectroscopy. Moreover, the optimized pulse shape can substantially enhance ultrafast semiconductor nonlinearities by almost a factor 4. This large enhancement makes adaptive feedback control interesting for optical switching schemes that use ultrafast semiconductor nonlinearities.[10,11]

Figure 1(a) shows the experimental setup, which consists of three main parts: a computer-based algorithm, a programmable pulse shaper, and a pump–probe setup for the acquisition of spectrally integrated (SI) differential transmission

(DT) data and DT spectra. The DT measurements provide the feedback signal for the algorithm, which optimizes the DT by changing the settings of the pulse shaper and the delay between pump and probe pulses. The three main parts
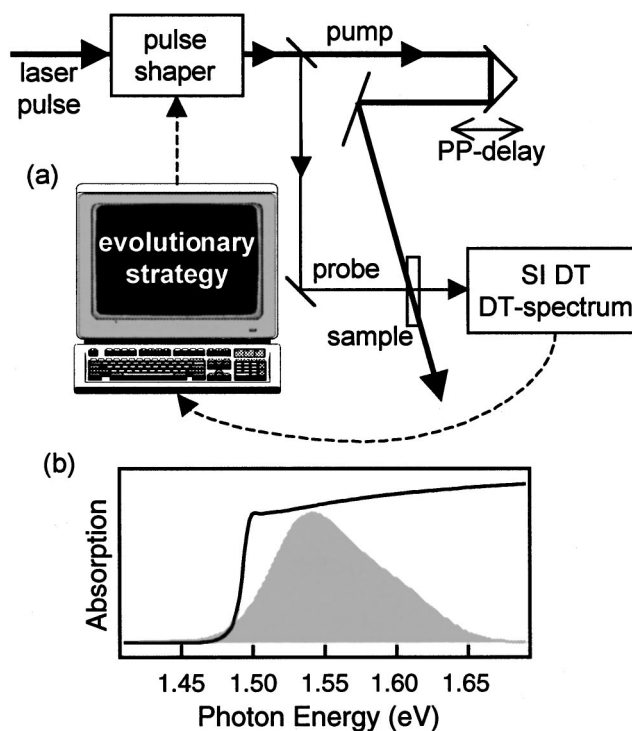


FIG. 1. (a) Experimental setup for adaptive feedback control of the spectrally integrated (SI) differential transmission (DT) and the DT in narrow spectral windows. Solid lines: optical beam path. The dashed lines illustrate how the feedback loop is closed between the experiment and the pulse shaper. Not shown: the computer-controlled evolutionary strategy also directs the pump–probe (PP) delay. In (b), the absorption spectrum of the $Al_{0.06}Ga_{0.94}As$ sample (solid curve) and the excitation pulse spectrum (shaded) are shown.

[a]Electronic mail: kunde@iqe.phys.ethz.ch

of the setup are described in more detail in the following.

Standard noncollinear DT measurements have been performed at room temperature with linearly cross-polarized pump and probe pulses from a Ti:sapphire laser. A programmable 4-$f$ pulse shaper[12,13] is positioned in front of the pump–probe beamsplitter so that both pulses experience the same modulation. The spectral components are filtered by a programmable pixelated liquid-crystal spatial light modulator (SLM) placed at the Fourier plane of the shaper. We have used the SLM to change only the spectral phase of the pulses without modification of the spectral amplitude. Pump and probe pulses have identical spectra, centered at 1.56 eV, with a spectral width sufficient to generate 20 fs pulses. The DT experiments have been carried out on a 1-$\mu$m-thick $Al_{0.06}Ga_{0.94}As$ bulk semiconductor sample. As seen in Fig. 1(b), mainly continuum transitions are excited in this sample. The excitation carrier density is $N_{exc} \approx 3 \times 10^{17}$ cm$^{-3}$ in all experiments.

As a global optimization procedure, an evolutionary strategy[14] is implemented for adaptive feedback control. This algorithm works with individuals carrying as genes the pump–probe time delay and either the parameters of a Taylor expansion of the spectral phase or the phase differences between adjacent pixels of the SLM. As a merit function, either the SI DT signal or the DT signal in a narrow spectral window is used. The evolutionary strategy maximizes the chosen merit function applying crossover, mutation, and selection[14] to find optimized values of the genes. For use as a spectroscopic tool, care has to be taken when choosing the genes. For each optimization problem, we have thoroughly checked the necessary number of genes for the phase by monitoring the merit function and the shape of the optimized phase. For each gene, the search space was adjusted as well as the parameters directing crossover and mutation.

After optimization, the spectral phase was characterized using two independent methods. First, we use second-harmonic-generation frequency-resolved optical gating (FROG).[15] Alternatively, the spectral phase can also be obtained from the settings of the pulse shaper. However, to get the actual phase $\varphi$ at the position of the sample, the shaper phase $\varphi_{shaper}$ has to be corrected for the phase $\varphi_{setup}$ of all other elements in the experimental setup, i.e., $\varphi = \varphi_{setup} + \varphi_{shaper}$. To determine $\varphi_{setup}$, we use the SLM for pulse compression. Following Refs. 3 and 4, we replace the semiconductor sample with a thin second-harmonic-generation (SHG) crystal (10 $\mu$m BBO) and let the adaptive feedback loop maximize the time-integrated SHG signal. After pulse compression, the shaper phase $\varphi_{SHG,max}$ compensates for $\varphi_{setup}$: $\varphi_{setup} = -\varphi_{SHG,max}$. We note that this phase characterization technique introduces a small error. According to Ref. 16, the maximization of the time-integrated SHG signal produces a constant temporal phase. For asymmetric spectra, this does not exactly correspond to a constant spectral phase. We have numerically checked that, in our experiments, this error is negligibly small. In fact, the results agree well with the FROG measurements.

In a first experiment, the adaptive feedback loop maximizes the SI DT. To explain the sensitivity of the SI DT to the spectral phase of the pump and probe pulses, we recall the results from Ref. 17. There, it has been demonstrated that
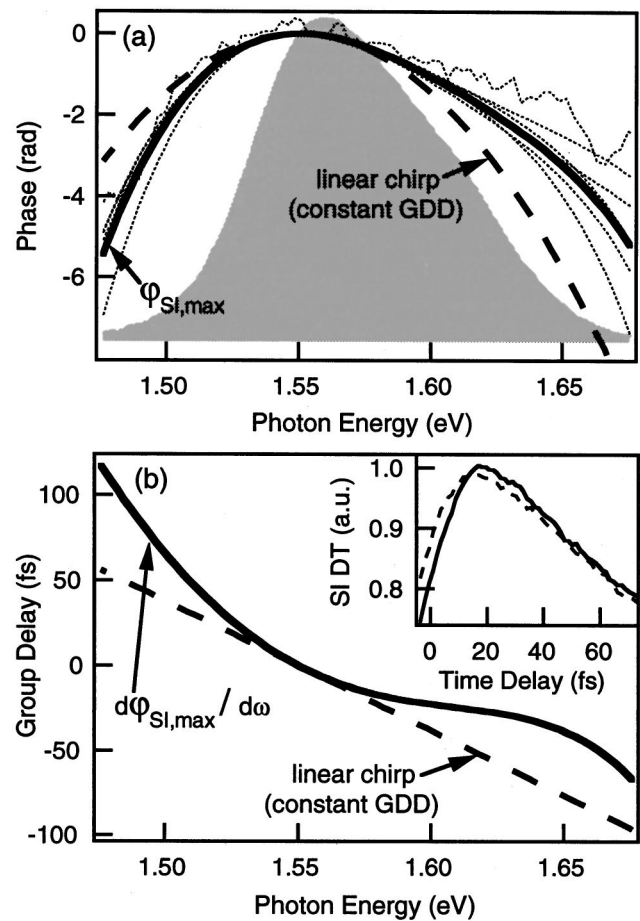


FIG. 2. (a) Average of several optimization runs (dotted curves) yields the optimum phase $\varphi_{SI,max}$ (solid curve), which maximizes the spectrally integrated differential transmission (SI DT). Shown for comparison: phase corresponding to a linear chirp, i.e., a constant group delay dispersion (GDD; dashed curve). Shaded: excitation pulse spectrum. Temperature 300 K. $N_{exc} \approx 3 \times 10^{17}$ cm$^{-3}$. (b) Group delay ($= d\varphi/d\omega$) obtained from $\varphi_{SI,max}$ (solid curve) as compared to a linear chirp (dashed curve). The inset shows the SI DT in arbitrary units for $\varphi_{SI,max}$ (solid curve) and for linear chirp (dashed curve).

linear downchirp enhances the SI DT as compared to linear upchirp or ''no chirp.'' Downchirp means that the high-energy components are in the leading edge of the pulse. A linear chirp corresponds to a constant group delay dispersion (GDD), i.e., $d^2\varphi/d\omega^2 =$ const. The intuitive picture developed in Ref. 17 shows that, in essence, downchirp is adapted to the changes of the DT spectrum during carrier thermalization: The center frequency of the optical pulses and the maximum of the DT spectrum both shift to lower energies with time, resulting in an enhancement of the SI DT. However, intuition fails to predict whether nonlinear downchirp leads to an even higher enhancement of the SI DT. Figure 2(a) shows the optimized spectral phases for different experimental runs. Although different in detail, all phases correspond to downchirp that significantly differs from a purely linear chirp. This is also visualized by the group delay ($= d\varphi/d\omega$) shown in Fig. 2(b). The shape of the phase that maximizes the SI DT gives an intuitive picture of the complex energy dependence of carrier relaxation in the thermalization regime. Therefore, the optimized spectral phase and the corresponding group delay in Fig. 2 reflect not only *that* the maximum of the DT spectrum shifts towards lower en-
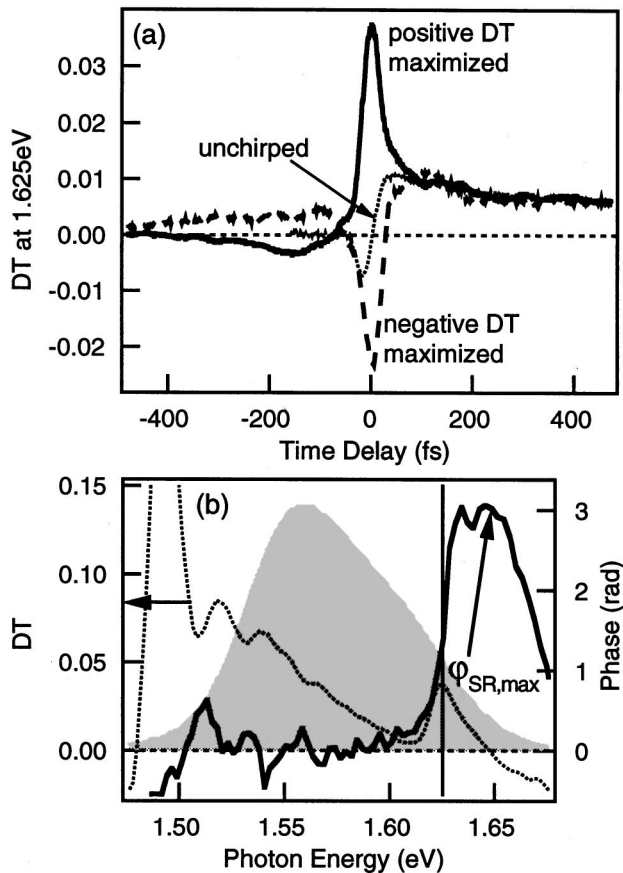
FIG. 3. (a) Differential transmission (DT) at 1.625 eV for unchirped pulses (dotted curve) and after maximizing the positive (solid curve) or the negative DT (dashed curve). $DT = \Delta T / T_0$ with $\Delta T$ pump-induced transmission change and $T_0$ transmission in absence of the pump. Temperature 300 K. $N_{\text{exc}} \approx 3 \times 10^{17}$ cm$^{-3}$. (b) Optimum phase $\varphi_{\text{SR,max}}$, which maximizes the DT at 1.625 eV and corresponding DT spectrum (dotted curve). Shaded: excitation pulse spectrum.

can also lead to negative DT.[19] This complex dynamics offers additional possibilities for adaptive pulse shaping schemes. As shown in Fig. 3(a), the positive DT can be enhanced by as much as a factor of $\approx 3.5$ compared to the DT for unchirped pulses. Around 1.625 eV, the optimized phase shows a rapid change of $\approx \pi$ and the corresponding DT spectrum exhibits a strong enhancement, as shown in Fig. 3(b). The phase change and the resonant-like enhancement reminds one of a driven-oscillator behavior. Alternatively, the feedback loop can maximize the negative DT. As shown in Fig. 3(a), the negative DT can also be amplified by a factor of more than 3. Hence, adaptive feedback control allows one to flip the sign of ultrafast semiconductor nonlinearities. A positive DT signal can be changed to a negative one, adjusting the spectral phase. Moreover, one can substantially enhance nonlinearities of either sign.

In summary, adaptive feedback optical pulse shaping allows one to control ultrafast semiconductor nonlinearities. Maximizing the spectrally integrated differential transmission, one obtains an intuitive picture of the complex energy dependence of carrier relaxation in the thermalization regime. Optimizing the differential transmission in a narrow spectral window, the sign and magnitude of ultrafast semiconductor nonlinearities can be substantially manipulated. These results show that adaptive feedback control of ultrafast semiconductor nonlinearities offers exciting possibilities for spectroscopy as well as for the optimization of ultrafast optical switching schemes.

ergies (corresponding to downchirp), but also *how fast* (shape of the downchirp) DT contributions in different spectral ranges shift towards lower energies. A slow variation of the group delay with energy corresponds to a fast shift of the DT spectrum. Hence, the group delay for the average optimum phase $\varphi_{\text{SI,max}}$ indicates that relaxation is faster at higher energies [see Fig. 2(b)].

We note that the overall difference in the SI DT magnitude between linear downchirp and the optimized phase is relatively small. As shown in the inset of Fig. 2(b), the SI DT is increased by only slightly more than 1%. This demonstrates that a carefully designed feedback optimization algorithm can be used as a sensitive tool in ultrafast spectroscopy. Although the changes in the merit function might be small, the shape of the optimized phase can give insight into the underlying interactions.

In a second experiment, we maximize the DT signal in a spectral window of 4 meV width at a photon energy of 1.625 eV. At this relatively high energy within the pulse spectrum, positive and negative DT can occur for unchirped pulses, as shown in Fig. 3(a). While the positive DT contributions can be attributed to phase-space filling, the negative DT contributions have been explained in terms of dynamic Fermi-edge singularity effects.[18] Moreover, coherent local-field effects

[1] J. Shah, *Ultrafast Spectroscopy of Semiconductors and Semiconductor Nanostructures*, 2nd ed. (Springer, Berlin, 1999).
[2] H. Haug and A.-P. Jauho, *Quantum Kinetics in Transport and Optics of Semiconductors* (Springer, Berlin, 1996).
[3] D. Yelin, D. Meshulach, and Y. Silberberg, Opt. Lett. **22**, 1793 (1997).
[4] T. Baumert, T. Brixner, V. Seyfried, M. Strehle, and G. Gerber, Appl. Phys. B: Lasers Opt. **B65**, 779 (1997).
[5] D. Meshulach, D. Yelin, and Y. Silberberg, J. Opt. Soc. Am. B **15**, 1615 (1998).
[6] R. S. Judson and H. Rabitz, Phys. Rev. Lett. **68**, 1500 (1992).
[7] C. J. Bardeen, V. V. Yakovlev, K. R. Wilson, S. D. Carpenter, P. M. Weber, and W. S. Warren, Chem. Phys. Lett. **280**, 151 (1997).
[8] A. Assion, T. Baumert, M. Bergt, T. Brixner, B. Kiefer, V. Seyfried, M. Strehle, and G. Gerber, Science **282**, 919 (1998).
[9] T. C. Weinacht, J. Ahn, and P. H. Bucksbaum, Nature (London) **397**, 233 (1999).
[10] R. Takahashi, Y. Kawamura, and H. Iwamura, Appl. Phys. Lett. **68**, 153 (1996).
[11] H. S. Loka and P. W. E. Smith, IEEE Photonics Technol. Lett. **10**, 1733 (1998).
[12] A. M. Weiner, D. E. Leaird, J. S. Patel, and J. R. Wullert, Opt. Lett. **15**, 326 (1990).
[13] M. M. Wefers and K. A. Nelson, J. Opt. Soc. Am. B **12**, 1343 (1995).
[14] H. P. Schwefel, *Evolution and Optimum Seeking* (Wiley, New York, 1995).
[15] K. W. DeLong, R. Trebino, J. Hunter, and W. E. White, J. Opt. Soc. Am. B **11**, 2206 (1994).
[16] T. Brixner, M. Strehle, and G. Gerber, Appl. Phys. B: Lasers Opt. **B68**, 281 (1999).
[17] J. Kunde, U. Siegner, S. Arlt, G. Steinmeyer, F. Morier-Genoud, and U. Keller, J. Opt. Soc. Am. B **16**, 2285 (1999).
[18] J.-P. Foing, D. Hulin, M. Joffre, M. K. Jackson, J.-L. Oudar, C. Tanguy, and M. Combescot, Phys. Rev. Lett. **68**, 110 (1992).
[19] K. El Sayed and C. J. Stanton, Phys. Rev. B **55**, 9671 (1997).